HHS Public Access

Author manuscript

Nat Neurosci. Author manuscript; available in PMC 2012 January 01.

Published in final edited form as:

Nat Neurosci. ; 14(7): 840–847. doi:10.1038/nn.2830.

KCNQ5 channels control resting properties and release probability of a synapse

Hai Huang[*] and **Laurence O. Trussell**

Oregon Hearing Research Center and Vollum Institute Oregon Health and Science University 3181 S.W. Sam Jackson Park Road, L335A Portland, Oregon 97239

SUMMARY

Little is known about which ion channels determine the resting electrical properties of presynaptic membranes. In recordings made from the rat calyx of Held, a giant mammalian terminal, we found that resting potential is controlled by KCNQ (Kv7) K^+ channels, most likely KCNQ5 (Kv7.5) homomers. Unlike most KCNQ channels which activate only upon depolarizing stimuli, the presynaptic channels began to activate just negative to rest. As a result, blockers and activators of KCNQ5 depolarized or hyperpolarized nerve terminals, respectively, markedly altering resting conductance. Moreover, the background conductance set by KCNQ5 channels, in concert with Na^+ and HCN channels, determined the size and timecourse of the response to subthreshold stimuli. Signaling pathways known to directly affect exocytic machinery also regulated KCNQ5 channels, and increase or decrease of KCNQ5 channel activity controlled release probability through alterations in resting potential. Thus, ion channel determinants of presynaptic resting potential also control synaptic strength.

Keywords

K^+ channel; calyx of Held; KCNQ; Kv7; axon terminals

The resting electrical properties of excitable cells are determined by a balance of tonic inward and outward currents. Outward ionic current is mainly contributed by K^+ channels and plays the dominant role in setting resting membrane potential (RMP) and conductance. The set point for this balance of currents is critical for determining the responsiveness of cells to excitation or inhibition. For example, background conductances of cells determine how effective stimuli are in altering membrane potential. Moreover, RMP determines the availability of channels that inactivate strongly, such as Na^+ and A-type K^+ channels. In nerve terminals, RMP has an additional function of controlling transmitter release probability, through weak activation of Ca^{2+} channels [1] or through Ca^{2+}-independent mechanisms [2]. Given the importance of resting properties to neurons, it is remarkable that

[*]**Address correspondence to:** Oregon Hearing Research Center and Vollum Institute 3181 S.W. Sam Jackson Park Road, Portland, Oregon 97239 huanghai@ohsu.edu.

Author Contributions: H.H. conducted and analyzed all experiments. L.O.T and H.H. designed experiments and wrote the manuscript.

very little is understood about the ion channels that determine membrane potential, particularly in presynaptic terminals.

While contributors to RMP have been examined in a variety of cell types [3-6] scant attention has been paid to what determines the resting properties of a synapse, in part because the small size of nerve terminals usually precludes direct measurement of presynaptic voltage. An exception is the calyx of Held, a giant glutamatergic terminal in the medial nucleus of the trapezoid body (MNTB), whose large size permits whole-cell patch-clamp recording [7, 8]. Resting inward ionic current results from I_h [8, 9] and persistent Na^+ current [10]. However, although previous studies showed that Kv1 and Kv3 channels contribute prominently to firing properties of the calyx [8, 11], blockers of these channels did not alter RMP. Thus, it remains unknown what K^+ channels set presynaptic RMP. Using pre- and postsynaptic recordings, combined with immunohistochemistry, we found that KCNQ5 (Kv7.5) channels with unusually negative activation voltage are expressed in the calyx. Given this voltage dependence, these channels accounted for the majority of resting outward ionic current and determined presynaptic resting conductance and release probability.

RESULTS

Identification of a K^+ current in the calyx of Held

Presynaptic voltage-clamp recordings were made to screen for K^+ channels active at subthreshold potentials. Initial recordings were performed in the presence of blockers of Na^+, Ca^{2+}, I_h, Kv1 and Kv3 channels (see Methods), which allowed us to examine the remaining ionic currents with better resolution, and also to clamp the membrane potential over a wider range of values. A slow voltage ramp (13 mV/s) evoked an outward current when the recording pipette contained a high K^+ solution (n=24), but not when pipette K^+ was replaced by Cs^+ (n=12, Fig. S1a), confirming that a K^+-channel mediated the outward current. Since the ramp was slow, this K^+ channel must not exhibit strong inactivation. We next used pharmacological approaches to identify the current. The outward current was relatively insensitive to 30 μM bupivacaine (Fig. S1b; 91±6% of control, p=0.19, n=5) or to extracellular pH change (Fig. S1c; 100±2% of control with pH change from 7.4 to 6.4, p=0.73, n=5; 99±1% of control with pH change from 7.4 to 8.4, p=0.62, n=4), manipulations which are known to block some two-pore K^+ channels [3]. Moreover, there was no effect of the hERG blocker E-4031 (10 μM; Fig. S1d; 101±2% of control, p=0.57, n=6). The outward current was partially blocked by puff application of 1 mM $BaCl_2$ (Fig. S1e; 42±6% of control at 0 mV after leak subtraction (see Methods), p=0.0003, n=7) or 1 mM 2-APB (Fig. S1f; 67±8% of control after leak subtraction, p=0.02, n=4). These agents, though antagonists of two-pore K^+ channel, were not considered selective enough to identify their targets. However, bath application of 10-20 μM XE991, a selective KCNQ antagonist, blocked almost all the outward current (Fig. 1a; left 12±2% after leak subtraction, p=0.0005, n=8). Another KCNQ blocker, linopirdine, had a similar effect, with 10 μM linopirdine suppressing the outward current to 17±4% after leak subtraction (Fig. 1b; p=0.008, n=4). These blockers removed about as much outward current as did K^+ replacement (Fig. S1a), indicating that the majority of the current was mediated by KCNQ channels. Consistent with this conclusion, the KCNQ ‘opener’ flupirtine (10 μM, Fig. 1c) potentiated outward current

by 21±3% after leak subtraction (p=0.009, n=5), as did the KCNQ agonist retigabine (5-10 μM, 41±4% increase, p=0.001, n=5).

Because receptors and channels may show transient expression during development, we monitored the amplitude of XE991-sensitive current using voltage ramps in rats from P9-18, a period associated with marked developmental changes related to onset of hearing [12]. The amplitude of KCNQ current varied widely among calyces, but on average increased up to P12, the age of hearing onset, and was maintained as late as P15-18 (see Fig. S2, p=0.04, ANOVA analysis), suggesting that KCNQ channels are expressed in mature synapses, consistent with immunohistochemical reports [13, 14].

Further analyses confirmed that KCNQ channels were restricted to the nerve terminal and were indeed the target of the drugs we applied. A previous immunohistochemical study showed KCNQ5 is probably expressed in calyces but, at least by P13, not in postsynaptic MNTB neurons [13]. We therefore tested the effects of XE991 on P10 & P16 MNTB principal neurons, which showed no expression of KCNQ5 protein, and found that even at 20 μM, XE991 did not affect postsynaptic K^+ currents, including those currents activated by stronger depolarization in the absence of any other channel blockers (Fig. S3). This result confirmed the selective presynaptic nature of channel expression, and indicated that XE991 was not blocking nonspecifically Kv1 or Kv3 channels, which are expressed pre- and postsynaptically [8, 11, 15, 16], and is consistent with the previous analysis of the drug's selectivity at 10-20 μM [17]. Although a higher concentration of XE991 can block ERG channels [18], E-4031-sensitive ERG channels are not expressed in calyx (Fig. S1d). Indeed, the magnitude of block obtained with 10 μM XE991 suggests it is effective at lower concentrations at which such nonspecific effects would be less likely. To confirm this we constructed a dose-inhibition curve for XE991 block of outward current (Fig. S4), finding an IC50 of only 3.9 μM. Thus, the presynaptic current blocked by XE991 is most likely mediated by KCNQ subunits.

Activation of presynaptic KCNQ current

The recordings in Fig. 1 were obtained in the presence of channel blockers, some of which, particularly TEA and 4-AP, might partially block KCNQ channels or subtly alter their properties [19]. We therefore re-examined XE991-sensitive current in the *absence* of other channel blockers. Although this recording condition limited how effectively we could control voltage upon depolarization, it allowed us to state more reliably at what potentials XE991-sensitive current is first detected and examine its properties near rest. A test 8-mV/s voltage ramp from −100 mV to −40 mV evoked an outward current, largely suppressed by 20 μM XE991 (Fig. 2a). By subtracting the trace in XE991 (gray trace) from the control trace (black trace), the current-voltage relation for KCNQ current (476±75 pA at −40 mV, n=7) was determined (Fig. 2b); from the enlarged KCNQ current trace (Fig. 2c), the threshold for *detection* of current (see Methods) was −83.1±1.0 mV (n=7). Boltzmann fits to conductance-voltage curves (Fig. 2d, dark gray trace) revealed a maximal conductance of 7.8±1.3 nS, a V_{Half} of −54.9±1.0 mV and a slope factor of 9.5±0.5 mV (n=7). These Boltzmann curves were limited by the range of voltages over which we could maintain clamp. To extend this rage sufficiently to obtain a full activation curve, we recorded in the

presence of Cd^{2+} and TTX, allowing us to clamp the terminal up 0 mV (Fig. 2e,f). The resulting Boltzmann fits were almost identical to those obtained in the absence of blockers.

Because these detection and activation potentials are quite negative to values reported previously [20-22], we also recorded KCNQ currents in hippocampal CA3 principal neurons, where KCNQ2/3 channels have been well described (see Fig. S5). The detection threshold in CA3 neurons were −64.4±2.2 mV. Boltzmann fitting showed a V_{Half} of −32.8±1.2 mV and the slope factor of 10.7±0.7 mV (n=5), similar to a recent study of these cells [20]. Both activation threshold and V_{Half} of the calyx were significantly negative to those of CA3 neurons ($p=9*10^{-6}$ and $p=6*10^{-8}$, respectively) while the slope is not significantly different (p=0.14). Note that the current blocked by XE991 has no linear, voltage-independent component (Fig. 2c,e), excluding the possibility that XE991 spuriously blocks a two-pore K^+ channel that might provide a resting leak current.

As an additional check on whether all outward ionic currents activating near −80 mV are KCNQ channels, we recorded the non-KCNQ K^+ current in the presence of Na^+, Ca^{2+}, I_h, and KCNQ blockers, and used TEA and 4-AP as a combined general blocker of any remaining outward currents. The threshold for detecting activation of TEA and 4-AP-sensitive current was −67.8±2.6 mV (Fig. S6, n=4), significantly more depolarized than for XE991-sensitive current (p=0.002).

Another characteristic of KCNQ is slow activation and deactivation, measured in response to voltage pulses [4, 21]. In the presence of Ca^{2+} channel blockers, a voltage-step from −80 to −40 mV evoked an outward current (Fig. 2g, black trace) which was reduced by XE991 (gray trace). The XE991-sensitive component, obtained by subtraction of these traces, was 464±64 pA and did not inactivate (Fig. 2h, n=6). The activation was best fitted with a double exponential whose fast and slow components were 44±9 ms and 627±146 ms, respectively, and the weighted mean was 237±34 ms (n=6). The slow component was 37± 5% of the fit (the remainder being fast component). Such slow kinetics and lack of inactivation are well-suited to determining the background conductance of synapses.

KCNQ5 subunits in the calyx

A previous study demonstrated KCNQ5 immunolabeling in excitatory synapses boutons in the auditory brainstem, including MNTB [13]; accordingly, mRNA for KCNQ5 is present in neurons of the cochlear nucleus, which contain cell bodies that give rise to calyceal terminals [14]. In pre-hearing animals (younger than P12), KCNQ5 was reported primarily in postsynaptic MNTB cells [14]. Since MNTB receives calyceal and non-calyceal inputs, as well as GABA- and glycinergic inhibition, we sought to establish that KCNQ5 was definitively in the calyx and also test the expression of other KCNQ subunits. We found indeed that antibodies to KCNQ5 intensely labeled domains between cell bodies in MNTB, suggestive of calyceal localization (Fig 3d). By contrast, antibodies to KCNQ2, 3 & 4 yielded nearly undetectable labeling (Fig 3a-c). As expected, KCNQ2 & 3 was detected in hippocampus [23, 24] and KCNQ4 was seen in cochlear nucleus [25] (data not shown). To confirm a calyceal site of expression of KCNQ5, calyces were patch clamped with pipettes containing biocytin. After termination of the recording, the slice was fixed, and double-labeled for biocytin and KCNQ5. As shown in Figure 3e-g, KCNQ labeling was prominent

in spaces between cell bodies, and clearly overlapped with the recorded calyx. Similar results were obtained in 3 slices. Postsynaptic principal cells labeled with biocytin did not exhibit KCNQ5 labeling (Fig. 3h-j), consistent with the absence of postsynaptic KCNQ current (Fig. S3). Given the very low expression of KCNQ2-4, these results demonstrate that XE991-sensitive current is likely generated by channels composed solely of KCNQ5 subunits.

The conclusions based on immunohistochemistry were confirmed by a pharmacological approach. Recent studies have identified compounds whose effects differ qualitatively among different KCNQ subunits. Presynaptic K^+ current was measured under conditions in which almost all current is XE991 sensitive (Fig. 1a). Diclofenac is a KCNQ2-4 activator but a blocker of KCNQ5 [26]. We found that 100 μM diclofenac inhibited the presynaptic K^+ current by 53±4% at 0 mV (Fig. 3k; p=0.004, n=5). Among cloned KCNQ subunits, UCL2077 is reported to inhibit all but KCNQ5, which exhibits voltage dependent potentiation by the drug [27]. UCL2077 at 10 μM potentiated K^+ current by 8±2% at 0 mV (Fig. 3l; p=0.05, n=4). Although it is controversial whether KCNQ1 is present in the CNS [28], this subunit does not have a profile of sensitivity to diclofenac or UCL2077 resembling that of the presynaptic current [26, 27]. These results support our immunohistochemical observations and indicate that the presynaptic KCNQ subunit is likely to be KCNQ5.

KCNQ contributes to resting properties of synapses

The RMP of the calyx of Held is typically −70 mV to −80 mV [7, 10, 11]. Given that we first detect activation of KCNQ current at −83 mV, it would be expected that some channels should be open at the RMP and thereby contribute to resting potential and conductance. Indeed, in current clamp and without other blockers, bath-application of 10 μM XE991 depolarized the membrane by 5 mV (Fig. 4a and c; from −75.4±0.9 mV to −70.9±1.0 mV, p=0.0009, n=8) and decrease the resting membrane conductance by 34% (Fig. 4d; from 4.9±0.9 nS to 3.2±0.6 mV, p=0.009, n=7). By contrast, 10 μM flupirtine hyperpolarized the membrane potential by 7 mV (Fig. 4b and d; from −75.1±1.5 mV to −82.9±1.7 mV, p=0.003, n=4) and increase resting membrane conductance by 256% (Fig. 4e; from 4.5±1.1 nS to 15.9±3.9 nS, p=0.03, n=4).

If KCNQ is the dominant resting presynaptic K^+ channel, why does XE991 depolarize the membrane potential by only 5 mV? We reasoned that a second K^+ channel, with a more positive activation range, could open when XE991 is applied, and thus oppose any further depolarization. The calyx of Held expresses several low-voltage activated Kv1 subunits that are sensitive to the antagonist margatoxin [8, 11]. As shown in Fig. 4h & i, margatoxin had no significant effect on the resting membrane potential (10 nM, average change +1.4±0.9 mV, p=0.23, n=4). However, when XE991 was applied first (10 μM, average change +5.2±0.8 mV, p=0.003, n=4) followed by margatoxin, the membrane depolarized by 19.2±1.4 mV (p=0.0002, n=5), and often triggered a brief bursts of spikes (Fig. g, i). Thus, KCNQ channels hold the membrane at negative potentials , thus minimizing significant contributions from other outward currents.

What other channels contribute to the resting conductance of the terminal? A likely source is HCN channels [8, 9], and thus we measured the drop in conductance induced by the HCN antagonist ZD7288. Bath application of ZD7288 (10-20 μM) decreased resting conductance from 4.5± 0.7 nS to 2.7± 0.6 nS, an average drop of 37±4% (p=0.003, n=4; data not shown). In a previous study [10], we found that persistent Na^+ current (NaP) contributed 27% of the resting conductance. Thus, these three channels (KCNQ, HCN, NaP) together account for 98% of the resting conductance of the terminal.

KCNQ currents modulate subthreshold signals

Nerve terminals may be depolarized by subthreshold signals as well as by action potentials. Presynaptic subthreshold voltage changes may arise from dendritic signals that propagate passively to axon terminals, where they regulate transmitter release [2]. Furthermore, calyces express glycine and $GABA_A$ receptors [29, 30], and activation of these receptors depolarize the membrane and increase transmitter release. Given the negative activation range for KCNQ, we predicted that any subthreshold voltage change would be modulated by these channels. Indeed, at the RMP, puffs of the $GABA_A$ agonist isoguvacine (200 μM) generated a depolarization whose amplitude was potentiated (p=0.04) and whose decay was slowed (p=0.004) by bath application of 10 μM XE991 (Fig. 5a-c; n=4). To test how KCNQ modulates the subthreshold responses under more controlled conditions, we injected calyces with current waveforms of different amplitudes to generate slow potentials (Fig. 5b-e). Application of 20 μM XE991 resulted in an increase in the amplitude (by 16-52%) and width (by 32-64%) of the current response (Fig. 5f-g). These results indicate that the effectiveness of subthreshold signaling in the axon terminal will be regulated by the activity of KCNQ.

Metabolic control of KCNQ5

It is well established that phosphatidylinositol-4,5-bisphosphate (PIP_2) is required for activation of KCNQ and that control of PIP_2 levels underlies muscarinic inhibition of KCNQ2/3 [31]. While we did not identify specific neuromodulators controlling KCNQ5 in calyces, it remained possible that signaling pathways responsible for the maintenance and regulation of exocytic machinery could also influence the electrical state of synapses. A candidate molecule is PIP_2. Besides its well-known regulation of ion channels, PIP_2 also plays a key role in control of proteins required for exocytosis [32, 33]. Moreover, electrical activity regulates PIP_2 levels in nerve terminals [34]. Therefore, it is possible that presynaptic KCNQ5 could be part of a complex of functional targets of PIP_2 that regulate exocytosis. We therefore asked if pharmacological reduction of PIP_2 levels inhibited KCNQ5 current in the calyx. Bath application of phenylarsine oxide (PAO, 30-100 μM), a phosphatidylinositol 4-kinase (PI4K) inhibitor which blocks the resynthesis of PIP_2 [35], reduced KCNQ current to 43±2% of control, measured at 0 mV using a ramp protocol (Fig. 6a-b, p=0.006, n=5). Weaker effects were observed with quercetin, another PI4K inhibitor (reduction to 77±6% of control, P=0.04, n=4) [36]. Application of PAO in the presence of XE991 generated no change in holding current, indicating that all of PAO's effects were due to KCNQ inhibition. PAO also change the voltage dependence and kinetics of presynaptic KCNQ current. Conductance-voltage relationships constructed from the response to voltage pulses as in Fig 6b,c revealed that the half-activation voltage and Boltzmann slope were shifted positive

(p=0.0001) and reduced (p=0.0008) respectively by PAO (control: $V_{1/2}$ −51.0±0.2 mV, k=9.2±0.1; PAO: −41.0±0.8 mV, k=13.0±0.6). Activation time constants for a depolarization from −80 mV to −40 mV accelerated in PAO (control: tau fast 35±7 ms, tau slow 447±122 ms (39% slow); PAO: tau fast 19±1 ms, tau slow 220±78 ms (30% slow), p=0.03, n=4). These results suggest that control of presynaptic PIP_2 levels would be expected to affect exocytosis through complex mechanisms, mediated through control of vesicle fusion and trafficking as previously described, but also electrically through KCNQ5.

Recent studies have indicated that KCNQ channels are also controlled by protein kinase C (PKC), which is targeted to the channel by A-kinase anchoring protein AKAP 150/79 [37]. The PKC activator, phorbol 12-myristate 13-acetate (PMA, 1-5 μM), was applied to determine whether PKC activation could regulate activity of presynaptic KCNQ5. As shown in Figure 6d and e, PMA reduced the KCNQ current to 56±3% of control (p=0.001, n=6). No effect was seen on currents in the presence of 10 μM XE991 (not shown). No effect of PMA on outward current was observed when a PKC inhibitory peptide was included in the patch pipette ($PKC_{19\text{-}31}$, 10 μM; p= 0.26, n=4) during recording. Unlike the results with PAO, no effect of PMA was observed on the conductance-voltage relation (control: $V_{1/2}$= −52.6±0.2 mV, k=9.2±0.1, n=4; PMA: $V_{1/2}$=−52.5±0.5 mV, k=11.0±0.5) or activation rates (not shown, p=0.74, n=4), suggesting PIP_2 and PKC act via distinct mechanisms [38, 39]. Together, these data show that PIP_2 and PKC regulate presynaptic KCNQ.

KCNQ decreases transmitter release probability

XE991 application depolarized the terminal by ~5 mV. Since previous studies of calyx established that small changes in RMP can alter transmitter release probability [1, 29] we tested the contribution of KCNQ to setting release probability. Postsynaptic cells were voltage clamped and presynaptic axons were stimulated with an extracellular electrode to evoke 2 EPSCs 20-ms apart. As shown in Figure 7a-c, application of 10 μM XE991 increased the first EPSC by 59±14% (p=0.03, n=7). Consistent with a change in transmitter release, XE991 decreased the paired-pulse ratio by 21% (Fig. 7c; from 0.94±0.11 to 0.74±0.11, p=0.000002, n=7). As mentioned above, XE991 had no effect on postsynaptic K^+ current, excluding that the change in EPSC amplitude could reflect alterations in security of voltage clamp. In contrast to the effect of XE991, application of 10 μM flupirtine decreased the first EPSC by 13±4% (Fig. 7d; p=0.04, n=4). A previous study showed that synaptic transmission in the calyx of Held under *in vivo*-like spontaneous activity levels could be quite different than in brain slices without such activity [40]. We therefore mimicked the conditioning effect of spontaneous activity by stimulating at 20 Hz for 10 s and then shifting to high-frequency stimuli (100 Hz). XE991 increased all EPSCs, either before or after the background activity (Fig. 7e). Indeed after 10-s conditioning stimuli, XE991 increased EPSC amplitude by 32±10% (p=0.009, n=4). The paired-pulse ratio was decreased by 13% (from 1.21±0.07 to 1.05±0.04, p=0.05, n=4). Thus, KCNQ-dependent determination of presynaptic resting properties is a significant factor in setting transmitter release probability regardless of spontaneous activity levels.

DISCUSSION

This study shows that KCNQ5 is a major contributor to the resting conductance of a mammalian nerve terminal. KCNQ, and in particular KCNQ5, was identified on the basis of the selective effects of 3 channel blockers (XE991, linopirdine, diclofenac), 3 channel openers (retigabine, flupritine, UCL2077), immunohistochemical screening for all four CNS subunits, as well as effects of PIP_2 and PKC inhibition consistent with previous reports. Outward current through presynaptic KCNQ5 is opposed by two sources of inward current, I_h [8, 9] and persistent Na^+ current [10]. An additional, activity dependent, source of outward current in the calyx is the Na,K-ATPase [9]. Together, these channels and the pump set RMP and indirectly control the responsiveness of the synapse to physiological stimuli.

Membrane potential, K^+ channels, and exocytosis

Studies in diverse species show that transmitter release is sensitive not only to the shape of the presynaptic spike but also to the RMP just prior to arrival of the spike [1]. This latter effect may arise from Ca^{2+}-dependent and Ca^{2+}-independent mechanisms [1, 2], and is likely to account for the ability of presynaptic GABA/glycine receptors or passive voltage signals from cell bodies to enhance exocytosis. In the calyx, where presynaptic Cl^- is elevated [29], GABA and glycine depolarize the membrane and increase release probability, an effect enhanced by the action of persistent Na^+ current [10]. K^+ channels can oppose this effect in several ways, by shunting, keeping the voltage negative to Ca^{2+} channel activation potentials, or narrowing the presynaptic spike, the latter effect counteracting any enhancement in release probability by background Ca^{2+}. Indeed, we observed that KCNQ opposed the depolarization evoked by a $GABA_A$ agonist. In principle, these effects could depend on the precise location of the channels. For background K^+ channel activity in presynaptic *en passant* boutons, the level of channel expression at synapses close to the cell body may affect exocytosis at those boutons, but also significantly affect spread of suprathreshold and subthreshold signals along distal portions of the axon. In this way, K^+ channels may both shape the action potential, and serve to control the spread of signals along axonal arbors. Identification of KCNQ5 in a variety on non-calyceal boutons makes this a likely possibility [13], particularly if the channels have activation properties like those identified here.

KCNQ and control of membrane properties

KCNQ channels have widespread function in the nervous system. KCNQ2/3 is expressed in hippocampus, especially in axon initial segments and mossy fibers [23, 24]. Several features of KCNQ2/3 conspire to determine the physiological function of the current, in particular their slow gating kinetics and their activation at potentials close to the RMP of postsynaptic cells, typically, −60mV to −70 mV. Blockade of KCNQ current by drugs or neurotransmitters depolarizes neurons, markedly enhances of excitability, and reshapes spike afterhypolarization [6].

Presynaptic KCNQ has received less attention. KCNQ2 has been identified in neuropil, suggesting the potential for a presynaptic function [23]. Indeed, activators and blockers of KCNQ modulate release of transmitters from synaptosome preparations [41]and affect

frequency of spontaneous miniature synaptic currents [42]. In cochlear hair cells, KCNQ4 may control background Ca^{2+} levels, and could in principle affect exocytosis [5]. A different conclusion was reached by Vervaeke et al. [43], who examined effect of XE991 and the activator retigabine on synaptic transmission in CA1 neurons of the hippocampus. In that study, application of XE991 only changed exocytosis when synapses were pre-depolarized by elevated bath K^+, indicating that the channels are not activated at the normal presynaptic RMP. Moreover, the effect of activators and blockers were to increase and decrease, respectively, EPSPs, results opposite to what might be expected for a presynaptic K^+ channel. The results were interpreted as an effect on Na^+ channel availability; hyperpolarizing the terminal by retigabine could increase the amplitude of the action potential and thus increase exocytosis.

By contrast, we find that KCNQ plays a significant role in calyceal terminal function in normal extracellular K^+, a result dependent entirely on the more negative activation voltage of the presynaptic channels. Unlike the case in synapses on CA1 neurons [43], calyceal channels are dominated by KCNQ5 subunits. However, this difference alone cannot explain the distinct biophysical properties, since KCNQ2-3 and 5 do not differ markedly in their activation or $V_{1/2}$ in heterologous expression systems [19, 21, 44]. KCNQ splice variants have been identified which differ in activation [45]. Moreover, membrane targeting proteins alter the susceptibility of KCNQ2-5 to muscarinic modulation [46], and it is likely that other properties of the channels could be regulated by accessory proteins or protein kinases. Interestingly, for KCNQ4, a subunit common in the peripheral auditory system, large differences in activation voltages between native and heterologously expressed channels has been attributed to differential phosphorylation and to coupling of channels to the motor protein prestin [47].

We observed that presynaptic KCNQ currents are reduced after lowering PIP_2 levels or activating PKC; both effects would be expected to result in enhanced release probability. However, PIP_2 and PKC are also associated with direct modulation of the exocytic machinery [32, 48]. Moreover, phorbol esters directly affect Munc13s, independently of PKC [49]. Thus, our results indicate that studies examining the effects of PIP_2 inhibitors and PKC activators on spike-driven exocytosis cannot be interpreted solely in terms of regulation of the SNARE complex. Rather, metabolic control of the nerve terminal may modulate simultaneously electrical and biochemical targets, and the balance of these effects will determine the change in transmitter release.

KCNQ subserves auditory function

KCNQ5 has received relatively little attention to date since it is not associated with muscarinic signaling and has not yet been identified as the basis for channelopathies [4, 19, 44]. However, like KCNQ4 [25], its prominence in auditory system [13] suggests that it confers a particular advantage in maintaining high-frequency synaptic signaling. If so, this would be consonant with the many molecular and biophysical specializations for preserving timing of electrical signals associated with sound [50]. Given the prevalence of this subunit throughout auditory brainstem regions, it is likely that the properties we described for the calyx will be common to many synapses. In particular, the more hyperpolarized activation voltage, which

contributes to a more negative RMP, has several clear physiological consequences. A more negative RMP will increase the availability of voltage-gated Na^+ channels, thus lowering spike threshold and increasing its amplitude. Moreover, a hyperpolarized RMP will increase the driving force for Ca^{2+} current after the spike. Both of these actions should contribute uniform and strong Ca^{2+} signals for exocytosis, necessary for the short-latency and consistent transmission that characterizes MNTB [50] and, more generally, make this channel well-suited to circuits in which fast axonal spiking plays a major role in signaling.

METHODS

Slice Preparation

The handling and care of animals was according to procedures approved by the OHSU. Coronal slices of brainstem containing the medial nucleus of the trapezoid body (MNTB) were prepared from 8- to 18-day-old Wistar rats [1, 10]. Briefly, 180–200 μm thick sections were prepared in ice-cold, low-Ca^{2+}, low-Na^+ saline using a vibratome (VT1200S; Leica). Immediately after the slices were cut, they were incubated at 35°C for 30–60 min in normal ACSF and thereafter stored at room temperature. The saline for slicing contained (in mM) 230 sucrose, 25 glucose, 2.5 KCl, 3 $MgCl_2$, 0.1 $CaCl_2$, 1.25 NaH_2PO_4, 25 $NaHCO_3$, 0.4 ascorbic acid, 3 *myo*-inositol, and 2 Na-pyruvate, pH 7.4 bubbled with 5% CO_2/95% O_2 . The ACSF for incubation and recording contained (in mM) 125 NaCl, 25 glucose, 2.5 KCl, 1 $MgCl_2$, 2 $CaCl_2$, 1.25 NaH_2PO_4, 25 $NaHCO_3$, 0.4 ascorbic acid, 3 *myo*-inositol, and 2 Na-pyruvate, pH 7.4 bubbled with 5% CO_2/95% O_2.

Whole-Cell Recordings

Slices were transferred to a recording chamber and were continually perfused with ACSF (2–3 ml/min) at ~ 32 °C. Calyces and MNTB neurons were viewed using Dodt contrast optics and a 40× water-immersion objective (Olympus) with a Zeiss Axioskop-2 microscope and a Nikon oil-coupled condenser. Pipettes pulled from thick-walled borosilicate glass capillaries (WPI) and filled with recording solutions described below had open tip resistances of 3–5 MΩ and 2–3 MΩ for the pre- and postsynaptic recordings, respectively. Whole-cell current- and voltage-clamp recordings were made with a Multiclamp 700B amplifier (Molecular Devices, Foster City, CA). Calyx terminals and MNTB neurons were identified by their appearance in contrast optics and/or Alexa 594 fluorescence (10–20 μM). For presynaptic experiments or for MNTB and hippocampal CA3 neurons studied with voltage ramps and steps, pipettes contained (in mM) 110 K-gluconate, 20 KCl, 1 $MgCl_2$, 10 HEPES, 4 MgATP, 0.3 Tris-GTP, and 3 Na_2-phosphocreatine and 10 $Tris_2$-phosphocreatine (290 mOsm; pH 7.3 with KOH). For the presynaptic K^+-free experiments, the K-gluconate was substituted by the same concentration of Cs-methanesulfonate, and pH was adjusted with CsOH. For postsynaptic MNTB EPSC recording, pipettes contained (in mM) 108 Cs-methanesulfonate, 5 NaCl, 1 $MgCl_2$, 10 HEPES, 5 EGTA, 0.4 Tris-GTP, 4 Mg-ATP and 14 $Tris_2$-phosphocreatine and 3 QX-314 (289 mOsm, pH 7.3 with CsOH). One hundred μM D/L-AP5, 10 μM SR95531 and 1μM strychnine were added to the ACSF to block NMDA, GABA and glycine receptor-mediated currents. In pair-pulse experiments, 2–5 mM kynurenic acid was also added to reduce saturation AMPA receptors. Series resistances (6–25 MΩ) were compensated by 60%–80% (bandwidth 3 kHz). Signals were filtered at 10 kHz

and sampled at 20~50 kHz. In some experiments, to isolate presynaptic KCNQ currents in response to voltage ramps, $CdCl_2$ (200 μM), tetrodotoxin (500 nM), CsCl (1 mM) and 4-AP (2 mM), with or without TEA-Cl (5 mM) were added to ACSF substituting for NaCl with equal osmolarity to block the Ca^{2+}, Na^+, I_h, and Kv1 and Kv3 channels, respectively. Resting membrane potential (RMP) was determined in current clamp (zero holding current). Liquid junction potentials were measured for all solutions, and reported voltages are adjusted appropriately. The resting conductance was measured in current-clamp mode using current steps around the RMP. Leak subtraction was not employed in any of the figures. For some ramp experiments, leak current was subtracted in order to calculate the degree of block of voltage-dependent current by a drug. This was done by extrapolating a linear fit to current between −100 mV and −85 mV and subtracting the fitted line from the traces. Drugs were applied by pressure ejection or bath perfusion. Flupirtine was dissolved with DMSO and the final DMSO concentration was less than 0.1%. XE991, linopirdine and other drugs were stored as aqueous stock solutions at −20 °C. Drugs for electrophysiology were obtained from Tocris (XE991, linopirdine and flupirtine), Ascent (SR 95531, D/L-AP5 and TTX), and all others from Sigma.

Analysis

Data were analyzed using Clampfit (Molecular Devices, Sunnyvale, CA) and Igor (WaveMetrics, Lake Oswego, OR). The detection threshold for activation of KCNQ current was determined from 1 kHz-filtered ramp data by extrapolating a line fitted between −100 and −90 mV; the point of deviation from this line (typically by several pA to be obvious by eye) was considered as the point of detectable activation of KCNQ. Boltzmann functions were used to describe KCNQ activation: $G=G_{Max} / (1+\exp(-(V-V_{HALF}) / k))$, where G is conductance in nS, G_{Max} is the maximal conductance, V is the holding potential in mV, V_{Half} is the voltage for half-maximal activation in mV, and k is the slope factor in mV. The standard double exponential functions were used to describe KCNQ activation kinetics: $f(t)=A_1*e^{-t/\tau 1} + A_2*e^{-t/\tau 2} + C$, where A_1 and A_2 are the amplitudes of fast and slow exponential components; and τ_1 and τ_2 are the time constants each components, respectively. The weighted time constant (τ) is expressed: $\tau=(A_1*\tau_1 + A_2*\tau_2) / (A_1 + A_2)$. Statistical significance was established using paired and unpaired t-tests as indicated, except as noted. Data are expressed as mean±S.E.M.

Immunohistochemistry

For KCNQ subtypes experiments, anesthetized rats (P10) were transcardially perfused with warm PBS solution (0.1 M, pH 7.4), and followed by cold 4% formaldehyde in PBS. The brains were dissected out and then postfixed for overnight at 4°C with the same fixative, rinsed in PBS, sectioned at 40 μm on a vibratome, and then washed extensively in PBS. For biocytin experiments, either the calyx or MNTB neurons of (P10) brainstem slices were whole-cell dialyzed with 0.3% biocytin diluted in K-gluconate-based internal solution for >10 min. After loading, slices were fixed by 2 hr incubation in fixative at 4°C and then extensively washed in PBS. After washing, the tissues were incubated in block solution consisting of 3% normal goat serum, 1% bovine serum albumin (BSA), and 0.25% Triton-X100 in PBS for 1 hr at room temperature, followed by overnight incubation with one of the primary antibodies against KCNQ channels (rabbit anti-KCNQ2, 1:500, AB5595,

Chemicon; rabbit anti-KCNQ3, 1:500, AB5597, Chemicon; rabbit anti-KCNQ5, 1:1000, AB5599, Chemicon [13, 14]; or rabbit anti-KCNQ4, 1:500, gift from Dr. Bechara Kachar of NIDCD, NIH) diluted in block solution at 4°C. After primary antibody incubation, sections were washed and incubated for 2 hr at room temperature with Alexa Fluor 488 fluorescence-conjugated secondary antibody goat anti-rabbit (1:500, Invitrogen) and/or Alexa Fluor 568-conjugated streptavidin (1:2500, Invitrogen). After washing, sections were mounted on slides, dehydrated in ascending alcohols, and delipidized in xylenes. The tissue was then rehydrated and coverslipped using Fluoromount G medium (Southern Biotechnology Associates). Fluorescence images were acquired using a confocal microscope (Olympus FV1000) by sequential scanning of Alexa Fluor 488 and/or Alexa Fluor 568 signals using an oil-immersion objective (60× magnification, numerical aperture 1.42). In comparing labeling of different subunits, confocal settings and processing were identical. Lack of crosstalk between fluorescence channels was confirmed by examining tissue labeled with only one of each of the fluorescence. Image analysis was conducted using NIH ImageJ software.

Supplementary Material

Refer to Web version on PubMed Central for supplementary material.

Acknowledgements

We thank Drs. Veera Balakrishnan and Paul Brehm for comments, and Drs. Kevin Bender and Sidney Kuo for technical advice. Supported by NIH grant DC004450 to L.O.T.

References

1. Awatramani GB, Price GD, Trussell LO. Modulation of transmitter release by presynaptic resting potential and background calcium levels. Neuron. 2005; 48:109–121. [PubMed: 16202712]
2. Alle H, Geiger JR. Analog signalling in mammalian cortical axons. Curr Opin Neurobiol. 2008; 18:314–320. [PubMed: 18801430]
3. Torborg CL, Berg AP, Jeffries BW, Bayliss DA, McBain CJ. TASK-like conductances are present within hippocampal CA1 stratum oriens interneuron subpopulations. J Neurosci. 2006; 26:7362–7367. [PubMed: 16837582]
4. Brown DA, Passmore GM. Neural KCNQ (Kv7) channels. Br J Pharmacol. 2009; 156:1185–1195. [PubMed: 19298256]
5. Oliver D, Knipper M, Derst C, Fakler B. Resting potential and submembrane calcium concentration of inner hair cells in the isolated mouse cochlea are set by KCNQ-type potassium channels. J Neurosci. 2003; 23:2141–2149. [PubMed: 12657673]
6. Shah MM, Migliore M, Valencia I, Cooper EC, Brown DA. Functional significance of axonal Kv7 channels in hippocampal pyramidal neurons. Proc Natl Acad Sci U S A. 2008; 105:7869–7874. [PubMed: 18515424]
7. Forsythe ID. Direct patch recording from identified presynaptic terminals mediating glutamatergic EPSCs in the rat CNS, in vitro. J Physiol. 1994; 479(Pt 3):381–387. [PubMed: 7837096]
8. Dodson PD, Forsythe ID. Presynaptic K+ channels: electrifying regulators of synaptic terminal excitability. Trends Neurosci. 2004; 27:210–217. [PubMed: 15046880]
9. Kim JH, Sizov I, Dobretsov M, von Gersdorff H. Presynaptic Ca2+ buffers control the strength of a fast post-tetanic hyperpolarization mediated by the alpha3 Na(+)/K(+)-ATPase. Nat Neurosci. 2007; 10:196–205. [PubMed: 17220883]
10. Huang H, Trussell LO. Control of presynaptic function by a persistent Na(+) current. Neuron. 2008; 60:975–979. [PubMed: 19109905]

11. Ishikawa T, et al. Distinct roles of Kv1 and Kv3 potassium channels at the calyx of Held presynaptic terminal. J Neurosci. 2003; 23:10445–10453. [PubMed: 14614103]
12. Taschenberger H, von Gersdorff H. Fine-tuning an auditory synapse for speed and fidelity: developmental changes in presynaptic waveform, EPSC kinetics, and synaptic plasticity. J Neurosci. 2000; 20:9162–9173. [PubMed: 11124994]
13. Caminos E, Garcia-Pino E, Martinez-Galan JR, Juiz JM. The potassium channel KCNQ5/Kv7.5 is localized in synaptic endings of auditory brainstem nuclei of the rat. J Comp Neurol. 2007; 505:363–378. [PubMed: 17912742]
14. Garcia-Pino E, Caminos E, Juiz JM. KCNQ5 reaches synaptic endings in the auditory brainstem at hearing onset and targeting maintenance is activity-dependent. J Comp Neurol. 2010; 518:1301–1314. [PubMed: 20151361]
15. Dodson PD, Barker MC, Forsythe ID. Two heteromeric Kv1 potassium channels differentially regulate action potential firing. J Neurosci. 2002; 22:6953–6961. [PubMed: 12177193]
16. Song P, et al. Acoustic environment determines phosphorylation state of the Kv3.1 potassium channel in auditory neurons. Nat Neurosci. 2005; 8:1335–1342. [PubMed: 16136041]
17. Wang HS, et al. KCNQ2 and KCNQ3 potassium channel subunits: molecular correlates of the M-channel. Science. 1998; 282:1890–1893. [PubMed: 9836639]
18. Elmedyb P, et al. Modulation of ERG channels by XE991. Basic Clin Pharmacol Toxicol. 2007; 100:316–322. [PubMed: 17448117]
19. Schroeder BC, Hechenberger M, Weinreich F, Kubisch C, Jentsch TJ. KCNQ5, a novel potassium channel broadly expressed in brain, mediates M-type currents. J Biol Chem. 2000; 275:24089–24095. [PubMed: 10816588]
20. Leao RN, Tan HM, Fisahn A. Kv7/KCNQ channels control action potential phasing of pyramidal neurons during hippocampal gamma oscillations in vitro. J Neurosci. 2009; 29:13353–13364. [PubMed: 19846723]
21. Miceli F, Cilio MR, Taglialatela M, Bezanilla F. Gating currents from neuronal K(V)7.4 channels: general features and correlation with the ionic conductance. Channels (Austin). 2009; 3:274–283. [PubMed: 19690464]
22. Tatulian L, Delmas P, Abogadie FC, Brown DA. Activation of expressed KCNQ potassium currents and native neuronal M-type potassium currents by the anti-convulsant drug retigabine. J Neurosci. 2001; 21:5535–5545. [PubMed: 11466425]
23. Cooper EC, Harrington E, Jan YN, Jan LY. M channel KCNQ2 subunits are localized to key sites for control of neuronal network oscillations and synchronization in mouse brain. J Neurosci. 2001; 21:9529–9540. [PubMed: 11739564]
24. Devaux JJ, Kleopa KA, Cooper EC, Scherer SS. KCNQ2 is a nodal K+ channel. J Neurosci. 2004; 24:1236–1244. [PubMed: 14762142]
25. Kharkovets T, et al. KCNQ4, a K+ channel mutated in a form of dominant deafness, is expressed in the inner ear and the central auditory pathway. Proc Natl Acad Sci U S A. 2000; 97:4333–4338. [PubMed: 10760300]
26. Brueggemann LI, Mackie AR, Martin JL, Cribbs LL, Byron KL. Diclofenac distinguishes among homomeric and heteromeric potassium channels composed of KCNQ4 and KCNQ5 subunits. Mol Pharmacol. 2010
27. Soh H, Tzingounis AV. The Specific Slow Afterhyperpolarization Inhibitor UCL2077 Is a Subtype-Selective Blocker of the Epilepsy Associated KCNQ Channels. Mol Pharmacol. 2010; 78:1088–1095. [PubMed: 20843955]
28. Goldman AM, et al. Arrhythmia in heart and brain: KCNQ1 mutations link epilepsy and sudden unexplained death. Sci Transl Med. 2009; 1:2ra6.
29. Turecek R, Trussell LO. Presynaptic glycine receptors enhance transmitter release at a mammalian central synapse. Nature. 2001; 411:587–590. [PubMed: 11385573]
30. Turecek R, Trussell LO. Reciprocal developmental regulation of presynaptic ionotropic receptors. Proc Natl Acad Sci U S A. 2002; 99:13884–13889. [PubMed: 12370408]
31. Suh BC, Hille B. Recovery from muscarinic modulation of M current channels requires phosphatidylinositol 4,5-bisphosphate synthesis. Neuron. 2002; 35:507–520. [PubMed: 12165472]

32. Hay JC, et al. ATP-dependent inositide phosphorylation required for Ca(2+)-activated secretion. Nature. 1995; 374:173–177. [PubMed: 7877690]
33. Holz RW, et al. A pleckstrin homology domain specific for phosphatidylinositol 4, 5-bisphosphate (PtdIns-4,5-P2) and fused to green fluorescent protein identifies plasma membrane PtdIns-4,5-P2 as being important in exocytosis. J Biol Chem. 2000; 275:17878–17885. [PubMed: 10747966]
34. Micheva KD, Holz RW, Smith SJ. Regulation of presynaptic phosphatidylinositol 4,5-biphosphate by neuronal activity. J Cell Biol. 2001; 154:355–368. [PubMed: 11470824]
35. Wiedemann C, Schafer T, Burger MM. Chromaffin granule-associated phosphatidylinositol 4-kinase activity is required for stimulated secretion. EMBO J. 1996; 15:2094–2101. [PubMed: 8641275]
36. Cochet C, Chambaz EM. Catalytic properties of a purified phosphatidylinositol-4-phosphate kinase from rat brain. Biochem J. 1986; 237:25–31. [PubMed: 3026313]
37. Hoshi N, et al. AKAP150 signaling complex promotes suppression of the M-current by muscarinic agonists. Nat Neurosci. 2003; 6:564–571. [PubMed: 12754513]
38. Nakajo K, Kubo Y. Protein kinase C shifts the voltage dependence of KCNQ/M channels expressed in Xenopus oocytes. J Physiol. 2005; 569:59–74. [PubMed: 16179364]
39. Shapiro MS, et al. Reconstitution of muscarinic modulation of the KCNQ2/KCNQ3 K(+) channels that underlie the neuronal M current. J Neurosci. 2000; 20:1710–1721. [PubMed: 10684873]
40. Hermann J, Pecka M, von Gersdorff H, Grothe B, Klug A. Synaptic transmission at the calyx of Held under in vivo like activity levels. J Neurophysiol. 2007; 98:807–820. [PubMed: 17507501]
41. Martire M, et al. M channels containing KCNQ2 subunits modulate norepinephrine, aspartate, and GABA release from hippocampal nerve terminals. J Neurosci. 2004; 24:592–597. [PubMed: 14736843]
42. Peretz A, et al. Pre- and postsynaptic activation of M-channels by a novel opener dampens neuronal firing and transmitter release. J Neurophysiol. 2007; 97:283–295. [PubMed: 17050829]
43. Vervaeke K, Gu N, Agdestein C, Hu H, Storm JF. Kv7/KCNQ/M-channels in rat glutamatergic hippocampal axons and their role in regulation of excitability and transmitter release. J Physiol. 2006; 576:235–256. [PubMed: 16840518]
44. Lerche C, et al. Molecular cloning and functional expression of KCNQ5, a potassium channel subunit that may contribute to neuronal M-current diversity. J Biol Chem. 2000; 275:22395–22400. [PubMed: 10787416]
45. Xu T, et al. Roles of alternative splicing in the functional properties of inner ear-specific KCNQ4 channels. J Biol Chem. 2007; 282:23899–23909. [PubMed: 17561493]
46. Roura-Ferrer M, et al. Functional implications of KCNE subunit expression for the Kv7.5 (KCNQ5) channel. Cell Physiol Biochem. 2009; 24:325–334. [PubMed: 19910673]
47. Chambard JM, Ashmore JF. Regulation of the voltage-gated potassium channel KCNQ4 in the auditory pathway. Pflugers Arch. 2005; 450:34–44. [PubMed: 15660259]
48. Saitoh N, Hori T, Takahashi T. Activation of the epsilon isoform of protein kinase C in the mammalian nerve terminal. Proc Natl Acad Sci U S A. 2001; 98:14017–14021. [PubMed: 11717460]
49. Rhee JS, et al. Beta phorbol ester- and diacylglycerol-induced augmentation of transmitter release is mediated by Munc13s and not by PKCs. Cell. 2002; 108:121–133. [PubMed: 11792326]
50. Trussell LO. Synaptic mechanisms for coding timing in auditory neurons. Annu Rev Physiol. 1999; 61:477–496. [PubMed: 10099698]

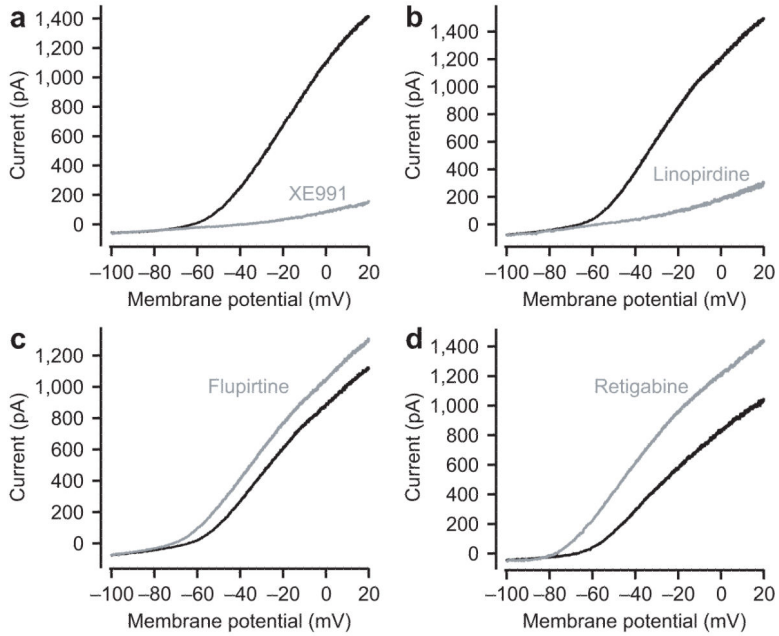

Fig. 1.

Identification of presynaptic KCNQ current. (**a**) A slow voltage ramp (13 mV/s) with a K^+-based internal solution evoked an outward current (black trace) that was strongly inhibited by 10-20 μM XE991, a KCNQ channel blocker (gray trace). The outward current was blocked by another KCNQ channel blocker linopirdine (**b**), while potentiated by KCNQ channel opener flupirtine (**c**) or retigabine (**d**). All traces were recorded in the presence of $CdCl_2$, tetrodotoxin, CsCl, 4-AP and TEA-Cl to block the Ca^{2+}, Na^+, I_h, and Kv1 and Kv3 channels (see Methods).

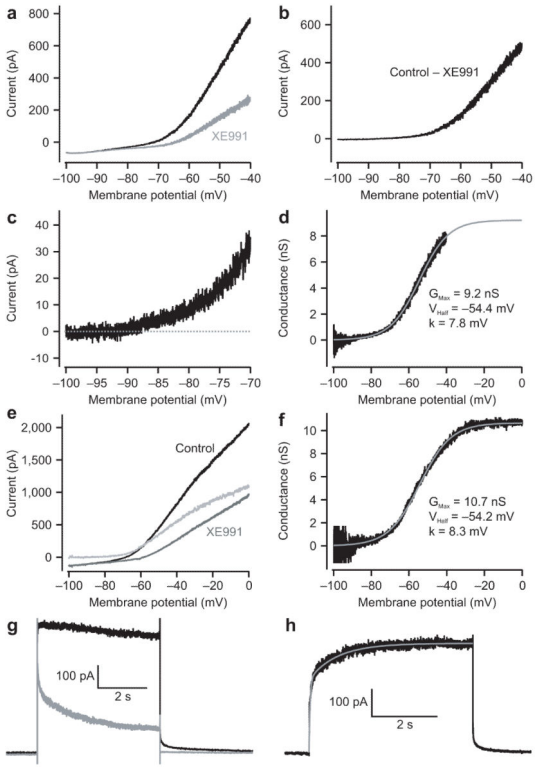

Fig. 2.

Voltage dependence of presynaptic KCNQ current. (**a**) A slow voltage ramp (8 mV/s) evoked an outward current (black) which was partially blocked by 20 μM XE991 (gray). (**b**) XE991-sensitive current from panel A (digital subtraction of gray from black trace in panel A). From the expanded figure (**c**), the activation KCNQ current is apparent at about −85 mV. (**d**) Conductance-voltage curve of the KCNQ current. Gray line is the Boltzmann fit. (**e**) Current-voltage relation in the presence of 200 μM Cd^{2+} and 1 μM TTX. Black: control, dark gray: 10 μM XE991, light gray: subtraction of XE991 curve from control curve. (**f**) Conductance-voltage curve of the KCNQ current from (e). Gray line is Boltzmann fit, with parameters as indicated. (**g**) Depolarizing pulse from −80 mV to −40 mV evoked an outward current recorded in the absence of channel blockers (black). The outward current is largely suppressed by XE991, leaving a smaller outward current with a fast inactivating component (gray). (**h**) XE 991 sensitive current obtained from the subtraction of traces in panel **g**. The current activation was fitted by an exponential function (gray line) with fast and slow components of 35 ms (67%) and 852 ms, and a weighted time constant of 308 ms.

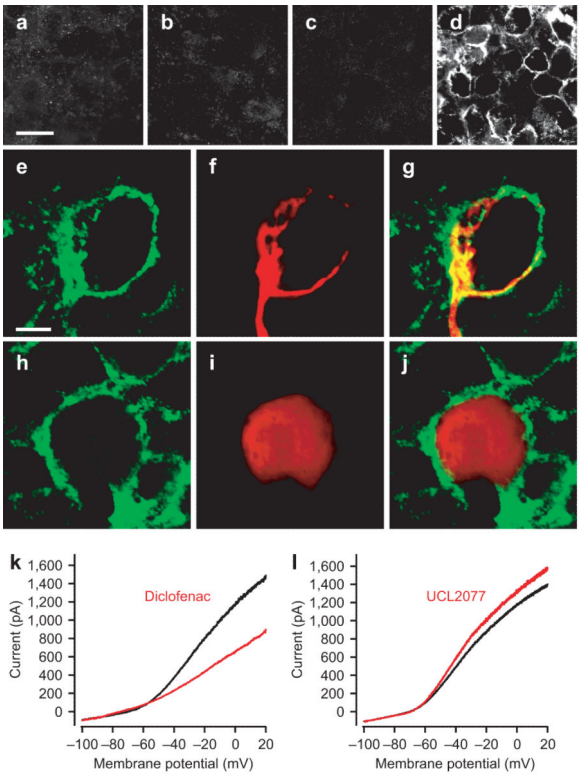

Fig. 3.

KCNQ5 is expressed in the calyx of Held. (**a-c**) show absence of labeling for KCNQ2-4, respectively, while panel **d** shows strong labeling for KCNQ5. Confocal settings were identical for panels a-d. (**e**) Labeling for KCNQ5 in a slice in which a calyx had been recorded and filled with biocytin (**f**). (**g**) Shows overlay of biocytin and KCNQ5 label, indicating that the channel is expressed in the calyx of Held. (**h**) In another slice, KCNQ5 labeling was performed after filling a postsynaptic cell (**i**) with biocytin. Overlay in (**j**) shows no postsynaptic somatic expression of the channel. Scale bar in (a) is 20 μm and applies to a-d; Scale bar in e is 5 μm and applies to panels e-f. The KCNQ current was inhibited by diclofenac (**k**) while potentiated by UCL2077 (**l**). All traces in g-h were recorded in the presence of $CdCl_2$, tetrodotoxin, CsCl, 4-AP and TEA-Cl to block the Ca^{2+}, Na^+, I_h, and Kv1 and Kv3 channels (see online Methods).

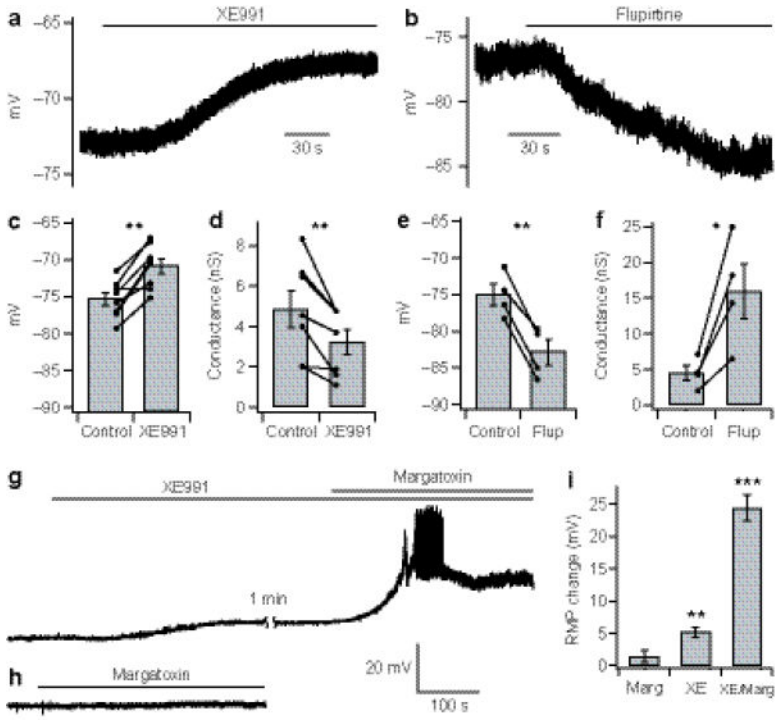

Fig. 4.

Effects of KCNQ channels on resting membrane properties of calyces. (**a**) Bath application of 10 μM XE991 depolarized resting membrane potential (RMP) by about 5 mV (n=8). (**b**) Bath application of 20 μM flupirtine hyperpolarized the RMP. (**c-d**) 10-20 μM XE991 depolarized the membrane and decreased resting conductance (n=7). (**e-f**) 20 μM flupirtine hyperpolarized the calyx and increased resting conductance (n=4). Conductance was estimated in current clamp with small positive and negative current steps around the RMP. (**g**) In the presence of 10 μM XE991, 10 nM margatoxin strongly depolarized the membrane. (**h**) Margatoxin by itself had no significant effect on the resting membrane potential. (**i**) Mean voltage changes produced by margatoxin, XE991, or margatoxin plus XE991. Voltage change induced by margatoxin alone was not significantly different from zero (p=0.23, n=4). Voltage changes induced by XE991 and by XE991 + margatoxin were significant (p=0.003, n=5 and p=0.0003, n=5 respectively), and were significantly different from one another (19.2±1.4 mV, p=0.002, n=5). Error bars show ± S.E.M..

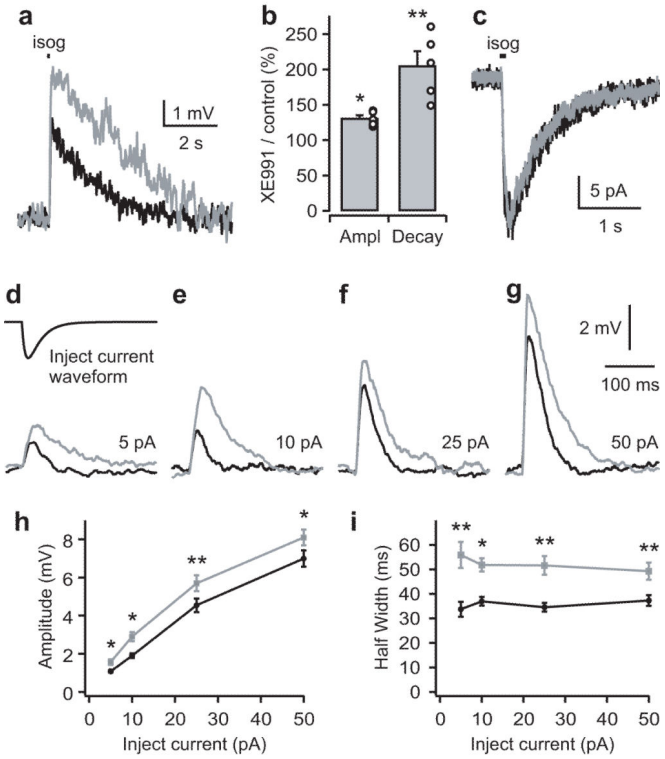

Fig. 5.

KCNQ channels determine properties of subthreshold stimuli. (**a-b**) Puff application of isoguvacine (0.2 mM, 100 ms) evoked depolarized responses (black trace), whose amplitude was potentiated and whose decay was slowed , by 10 μM XE991 (gray trace). (**c**) under voltage-clamp, isoguvacine-induced current was not affected by XE991. (**d-g**) Synaptic-like waveforms (rise time constant 7.5 ms, decay time constant 25 ms; black trace in d) of different amplitudes were injected into the calyx. Voltage responses are shown in black traces while gray traces show responses recorded with 10 μM XE991. Voltage response traces are averages of 4-8 applications. (**h-i**) Statistical data summarize XE991 effects on response amplitudes (h) and half width (i). Error bars show ± S.E.M..

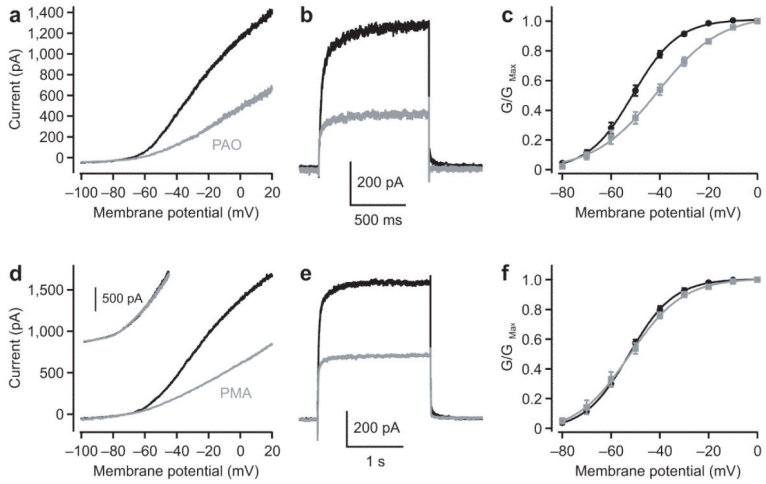

Fig. 6.

Modulation of KCNQ current by PIP_2 and PKC. (**a-b**) A slow voltage ramp (13 mV/s; a) or a voltage step from −80 mV to −30 mV (**b**) evoked an outward KCNQ current (black), which was partially inhibited by PI4 kinase inhibitor PAO (50 μM; gray). (**c**) PAO positively shifted the conductance-voltage curve. (**d-e**) 2 μM PMA, a potent protein kinase C activator, also inhibited the outward KCNQ current evoked by voltage ramp (**d**) or a voltage step (**e**). Inset in (d) shows that the PMA effects were blocked by PKC inhibitory peptide PKC_{19-31}. Voltage ramp was from −100 to +20 mV as in main panel. (**f**) PMA has no effects on conductance-voltage relationship. All traces were recorded in the presence of $CdCl_2$, TTX, CsCl, and 4-AP to block the Ca^{2+}, Na^+, I_h, and Kv1 and Kv3 channels. Boltzmann fit parameters given in text. Error bars show ± S.E.M..

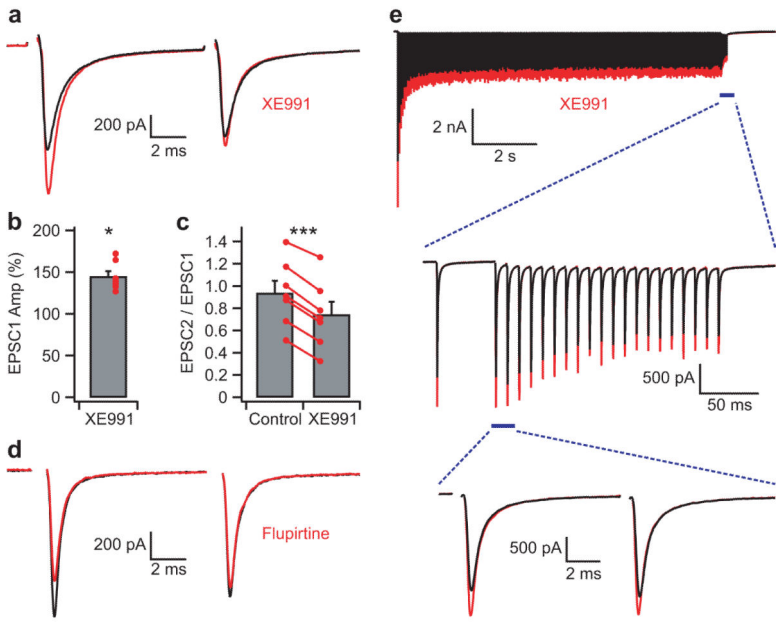

Fig. 7.

Regulation of transmitter release by KCNQ channels. (**a-b**) Application of 10 μM XE991 increased the first EPSC amplitude but has a smaller effect on the second EPSC in a pair-pulse protocol. (**c**) XE991 significantly decreased paired-pulse ratio. (d) Ten μM flupirtine decreased the first EPSC amplitude but with smaller effect on the second EPSC. (**e**) The calyx was first preconditioned by 20 Hz stimuli for 10 s, followed immediately by a period of 100 Hz stimuli. Ten μM XE991 increased all EPSCs but to different degrees. Each trace is an average of 4–10 recordings. Error bars show ± S.E.M..